(REVIEW ARTICLE)

Green synthesis of potent anticancer and antibacterial xanthene and chromene derivatives using agar as a catalyst: Molecular docking and in silico ADMET insights

Ali-Kakeshpour [1], Ashraf-Moradi [1, *] and Farzaneh-Moradi [2]

[1] Department of Chemistry, University of Zabol, Zabol, Iran.
[2] Department of Chemistry, University of Mazandaran, Babolsar, Iran.

Abstract

This study presents an innovative green synthesis method for xanthene, benzoxanthene, and chromene derivatives using agar as a natural catalyst. Our method achieves high yields (up to 95%) with short reaction times (less than 1 hour) under environmentally friendly conditions and simple work-up procedures.

The docking analysis conducted provides insights into the complex binding energies, molecular interactions, and hydrogen bond energies and distances. Molecular docking studies reveal strong chemical interactions with human serum albumin (HSA) and DNA gyrase, suggesting strong anticancer and antibacterial potential with binding energies ranging from -8.5 to -9.8 kcal/mol.

In silico ADMET analysis and drug-likeness analysis confirm favorable pharmacokinetic properties, including high oral bioavailability and low toxicity. This work offers a sustainable and effective approach to developing new therapeutic agents.

Keywords: Agar catalyst; Green chemistry; Anticancer agents; Antibacterial agents; Molecular docking; In silico ADMET

1. Introduction

With the increasing emphasis on environmental sustainability, the development of green chemistry methods for synthesizing biologically active compounds is of paramount importance [1-3]. Xanthene and chromene derivatives are prominent due to their diverse pharmacological activities, including anticancer and antibacterial properties. However, existing synthesis methods often involve toxic reagents and harsh conditions. Here, we report a green synthesis approach using agar, a natural and biodegradable catalyst, to produce these derivatives efficiently. Computational chemistry techniques, including molecular docking and *in silico* ADMET studies, were employed to explore the molecular interactions and pharmacokinetic properties of these compounds [4].

Our group's research on Agar was first published in 2015 [3]. Agar is derived from the polysaccharide agarose, which forms the supporting structure in the cell walls of certain species of algae. Generally, Agar is actually a resulting mixture of components: the linear polysaccharide agarose, agarose polymer, sugars such as galactose, gluconic acid, and xylose, Amino acids: Garyn, glutamic acid, threonine, and a heterogeneous mixture of smaller molecules called agaropectin. Chemically, agar is a polymer composed of subunits of the sugar galactose. This naturally occurring product contains numerous hydroxyl groups and therefore it can act as a mild catalytic system.

* Corresponding author: Ashraf Moradi

With the increase in environmental consciousness and demand for sustainable resources, the use of non-toxic and abundant catalysts in efficient preparation of organic compounds is sought. Natural biopolymers, equipped with various functional groups are suitable candidates for exploring new catalyst systems providing the possibility of performing reactions under mild conditions [5-10]. Currently, the world faces a plethora of health problems, with cancer and infectious diseases dominating [11]. Bacterial infections, in particular, pose a serious threat to human lives due to their emerging resistance to existing antibiotics, contributing to the growing public health problem. Therefore, the discovery of novel anticancer and antimicrobial agents is a crucial and timely endeavor for public health. Oxygen atom-containing heterocyclic molecules are among the main targets in drug design research. Chromene compounds, in particular, are well-known as important components in both biologically active synthetic and natural compounds [12, 13]. In this context, derivatives of Xanthene, Benzoxanthene, and 2-Amino-chromene represent significant classes of compounds, with applications ranging from pharmacology and medicine to the development of pH-sensitive fluorescent sensors and lasers [2, 14-27]. Despite the broad interest in these compounds, their current synthetic protocols suffer from many disadvantages associated with "non-green" chemistry. We herein report a practical, inexpensive, and safe method that utilizes commercially available and environmentally benign agar [5] as a superior catalyst for one-pot preparation of a plethora of functionalized 9,9-dimethyl-12-phenyl-9,10-dihydro-8H-benzo[a]xanthen-11(12H)-one and 14H-dibenzo [a,j] xanthene derivatives, as well as other similar derivatives shown in Figure 1.

A survey of the current literature reveals multiple reports on accessing these valuable compounds. However, many of these methods suffer from long reaction times, low yields, the use of hazardous heavy metal catalysts, reliance on multi-step strategies, the use of toxic organic solvents, and the formation of unwanted byproducts, necessitating tedious work-up procedures. For example, the synthesis of tetrahydrobenzo[b]xanthen-11-ones has been reported in the presence of ceric ammonium nitrate [28], $InCl_3$ and P_2O_5 [29] proline triflate [30] strontium triflate [31], and pipridine [32]. Additionally, the synthesis of 14H-dibenzo[a,j] xanthene has been reported by the condensation of β-naphthol and aldehydes in the presence of Amberlyst-15 [33], aluminium hydrogensulfate [34], sulfamic acid [35], p-toluenesulfonic acid [36], and cation-exchange resins [37]. Modified methods for the synthesis of amino-cromenes have also been reported using an amino-functionalized ionic liquid [38], cetyltrimethylammonium chloride [39] or bormide under ultrasound irradiation [40], as well as KF/Al_2O_3, [41] Na_2CO_3, [42] and DABCO [43].

Several studies have shown that the synthesized compounds exhibit individual anticancer activities through interactions with cancer-related receptors. Additionally, they can bind to human serum albumin (HSA), which plays a significant role in drug delivery. DNA gyrase is an enzyme within the class of topoisomerases that catalyzes changes in the topology of DNA. The presence of DNA gyrase in all bacteria except higher eukaryotes makes it a drug target for antibacterial studies [44, 45](4,5). Therefore, all compounds were docked to human serum albumin, and chromene-based compounds were docked to the DNA gyrase enzyme. Finally, *in silico* ADMET properties and drug-likeness analyses of the synthesized compounds were computed.

2. Experimental

2.1. Materials and equipment

All reagents were purchased from Merck, Fluka, or Aldrich and were used without further purification. NMR spectra were recorded on a Bruker Avance DPX 400 MHz spectrometer, with chemical shifts referenced using TMS. IR spectra were obtained using a JASCO FT-IR 460 Plus spectrophotometer. Melting points were determined in open capillaries using a BUCHI 510 melting point apparatus. TLC was performed to monitor all reactions, utilizing silica-gel Poly Gram SIL G/UV 254 plates.

2.2. General procedure for the synthesis of 14H-dibenzo[a,j] xanthene and tetrahydrobenzo [a]xanthen-11-one derivatives

A mixture of an aldehyde (1.0 mmol), β-naphthol (2b) (2.0 mmol) and agar (0.15 g) was added to a mixture of water/ethanol (3:1, 4 mL). Additionally, a mixture of an aldehyde (1.0 mmol), β-naphthol (2b) (1.0 mmol), dimedone (4) and agar (0.1 g) in ethanol was prepared. The reaction mixture was then stirred under reflux conditions for an appropriate period. The progress of the reactions was monitored by TLC. After completion of the reaction, the mixture was cooled to room temperature, diluted with water, filtered, and washed with distilled water. The crude product was recrystallized from ethanol to obtain the pure 14H-dibenzo [a,j] xanthene and 9,9-dimethyl-12-phenyl-9,10-dihydro-8H-benzo[a]xanthen-11(12H)-one derivatives. The purity of the products was confirmed by comparison of their physical data (melting points, IR, and 1H NMR) with those of known compounds in the literature [29-43, 46, 47].

2.3. General procedure for the synthesis of 2-amino-chromene and 2-amino-benzopyran derivatives (8-10, 12, 13)

A mixture of an aldehyde (1.0 mmol), malononitrile (1.0 mmol), an enolizable compound, and an activated phenol was stirred under reflux conditions. The progress of the reaction was monitored by TLC. All isolation and purification procedures were performed as described in the synthesis of xanthenes. The purity of the products was confirmed by comparison of their physical data (melting points, IR, and 1H NMR) with those reported in the literature [1, 38-43, 46-67].

2.4. Some spectral data for selected products are represented below

2.4.1. 14-(2,4-dichlorophenyl)-14H-dibenzo[a,j] xanthenes (A8):

m.p. = 229–230 °C; IR (KBr, cm^{-1}): 3059, 2919, 1619, 1591, 1558, 1514, 1457, 1408, 1239, 1206, 1135, 1101, 1047, 960, 865, 833, 806, 744, 696, 604; ^{1}H NMR (400 MHz, CDCl$_3$):

δ (ppm)= 6.6 (s, 1H, CH), 6.79 (d, 1H, CH), 7.17 (s, 1H, CH), 7.28 (d, 1H, CH), 7.39 (t, 2H, 2CH), 7.45 (d, 2H, 2CH), 7.6 (t, 2H, 2CH), 7.74 (d, 2H, 2CH), 7.80 (d, 2H, 2CH), 8.59 (d, 2H, 2CH).

2.4.2. 9,9-dimethyl-12-(4-Methoxyphenyl)-9,10-dihydro-8H-benzo[a] xanthen-11(12H)-one (B10):

m.p. = 201–204 °C; IR (KBr, cm^{-1}): 2950, 1646, 1597, 1372, 1227, 1185, 1027, 833; ^{1}H NMR (400 MHz, CDCl$_3$): δ (ppm) = 0.99 (s, 3H, CH$_3$), 1.13 (s, 3H, CH$_3$), 1.91 (s, 2H, CH$_2$), 2.26 (d, 1H, CH), 2.28 (s, 2H, CH$_2$), 2.32 (d, 1H, CH), 3.8 (s, 3H, OCH$_3$), 5.66 (s, 1H, CH), 6.89 (d, 1H, Ar-H), 7.20–7.37 (m, 4H, Ar-H), 7.73–7.77 (m, 2H, Ar-H), 8.02 (d, 1H, Ar-H).

2.4.3. 2-amino-4-(3-nitrophenyl)-5,10-dioxo-5,10-dihydro-4H-benzo [g]chromene-3-carbonitrile (C2):

m.p. = 236–238 °C; IR (KBr, cm^{-1}): 3458, 3354, 3190, 2925, 2199, 1664, 1594; ^{1}H NMR (400 MHz, CDCl$_3$): δ (ppm)= 5.06 (s, 1H, CH), 6.9 (s, 2H, NH$_2$), 7.69-8.41 (m, 8H, Ar-H).

2.4.4. 2-amino-4-(3-chlorophenyl)-4H-benzo[h]chromene-3-carbonitrile (D5):

m.p. = 228–231 °C; IR (KBr, cm^{-1}): 3455, 3340, 3023, 2930, 2210, 1645, 1600, 1580, 1470, 1378, 1266, 1030, 816, 750, 700; ^{1}H NMR (400 MHz, DMSO-d$_6$): δ (ppm)= 4.98 (s, 1H, CH), 7.15 (d, 1H, CH), 7.25 (s, 1H, CH), 7.26 (s, 2H, NH$_2$), 7.33–7.38 (m, 3H, 3CH), 7.55–7.64 (m, 3H, 3CH), 7.91 (d, 1H, CH), 8.29 (d, 1H, CH).

2.4.5. 3-amino-1-(4-nitrophenyl)-1H-benzo[f]chromene-2-carbonitrile (D,2):

m.p. = 184–187 °C; IR (KBr, cm^{-1}): 3472, 3325, 2190, 1650, 1610, 1582, 1540, 1502, 1340, 1244, 1200, 1056, 810; ^{1}H NMR (400 MHz, DMSO-d$_6$): δ (ppm)= 5.56 (s, 1H, CH), 7.25 (s, 2H, NH$_2$), 7.42 (d, 1H, CH), 7.44–7.63 (m, 2H, 2CH), 7.47 (d, 2H, 2CH), 7.71–8.03 (m, 2H, 2CH), 7.99 (d, 1H, CH), 8.17 (d, 2H, 2CH).

2.4.6. 2-amino-4-(4-nitrophenyl)-5-oxo-4,5-dihydropyrano[3,2-c]chromene-3-carbonitrile (E2):

m.p. = 265–268 °C; IR (KBr, cm^{-1}): 3476, 2190, 1720, 1612; ^{1}H NMR (400 MHz, DMSO-d$_6$): δ (ppm)= 3.15 (brs, 2H, NH$_2$), 4.63(s, 1H, CH), 7.25-8.01 (m, 8H, Ar-H).

2.4.7. 2-amino-4-(4-methoxyphenyl)-7,7-dimethyl-5-oxo-5,6,7,8-tetrahydro-4H-chromene-3-carbonitrile (F11):

m.p. = 172–173 °C; IR (KBr, cm^{-1}): 3432, 3328, 3212, 2198, 1678, 1599, 1502, 1211; ^{1}H NMR (400 MHz, DMSO-d$_6$):

δ (ppm)= 0.95 (s, 3H, CH$_3$), 1.1 (s, 3H, CH$_3$), 2.07 (s, 3H, CH$_3$), 1.95–2.36 (m, 4H, 2CH$_2$), 4.41 (s, 1H, CH), 5.80 (s, 2H, NH$_2$), 7.11–7.2 (m, 4H, Ar-H).

2.5. Molecular docking study

The docking process demonstrated significant docking scores and binding affinities of the synthesized compounds with the proteins human serum albumin (HSA) and DNA gyrase B. Molecular docking of the synthesized compounds into the 3D X-ray receptor structure was performed using the Smina program [68]. The 3D structures of the compounds were built using ChemDraw Pro 12.0 software and energy minimized. Crystal structures of human serum albumin (HSA) (PDB ID code: 1O9X) with a resolution of 3.2 Å and the antimicrobial agent Clorobiocin bound to topoisomerase II DNA gyrase B (E.coli 24 kDa N-terminal domain of DNA gyrase B) (PDB ID code: 1KZN) with a resolution of 2.3 Å were obtained from the RCSB Protein Data Bank (http://www.rcsb.org). Crystallographic waters and ligands were removed, and polar

hydrogens were added to the proteins. Molecular docking of all compounds (A1-A12, B1-B12, C1-C12. D1-D13, D,1-D,11, E1-E18, F1-F17) with HSA was then carried out. Additionally, we investigated the theoretical binding mode of compounds C1-C12, D1-D13, D,1-D,11, E1-E18, F1-F16 at the chlorobiocin binding site using molecular docking modeling. The binding features of synthesized chromenes with DNA gyrase were evaluated in a similar manner to the binding of chlorobiocin as a well-known enzyme inhibitor [69]. Molecular docking studies were performed for these ligands to understand the ligand-receptor possible intermolecular interactions in detail. During the docking studies into protein active sites, ligands were assumed to be flexible molecules, and the docking software was allowed to rotate all rotatable bonds of the ligands to obtain the best and optimized conformer within the active site of the enzyme using the biased probability Monte Carlo (BPMC) minimization procedure, which involved local energy minimization after each random move. The docking calculation in AutoDock Vina involved a number of sequential steps, including random perturbation of the conformation, local optimization using the Broyden-Fletcher-Goldfarb-Shanno algorithm, and a selection step in which the conformation was accepted or not [70]. Among the various conformations obtained from the docking procedure, the conformation with the lowest binding energy was selected for further analysis. The docking results were visualized using BIOVIA Discovery Studio client 2016. The interacting energies between each amino acid and the best pose of the docked compounds into the protein binding site were calculated using Molegro Molecular Viewer 2.5 (MMV) (http://www.molegro.com/mmv-product.php).

Molecular docking was performed using Smina with the crystal structures of HSA (PDB ID: 1O9X) and DNA gyrase B (PDB ID: 1KZN). The binding affinities and interactions were analyzed using BIOVIA Discovery Studio.

2.6. *In silico* ADMET study

For the theoretical prediction of pharmacokinetic properties, including absorption, distribution, metabolism, excretion, and toxicity (ADMET) of the compounds, and drug-likeness, we utilized the OSIRIS DataWarrior version 4.6.1 and QikProp version 3.2 programs (Schrödinger, Portland, OR, USA, 2009) (http://www.schrodinger.com/QikProp). In the toxicity risk assessment, the molecular fragments responsible for these effects were identified by designing valid chemical structures. Four characteristics related to the compound were investigated and classified as risks (high, none, or low) regarding mutagenicity, tumorigenicity, irritancy, and reproductive effects. Drug-likeness, a quality concept used in drug design methodology, was also computed [71-73].

3. Results and discussion

3.1. Chemistry

To determine the optimal conditions for efficiently preparing 14H-dibenzo [a,j] xanthene derivatives, we conducted the reaction of 4-chlorobenzaldehyde (1.0 mmol) and β-naphthol (2.0 mmol), as a model reaction. The results are summarized in Table 1. In the absence of a catalyst, only trace amounts of the desired product 3e were obtained, even after a long reaction time (Table 1, entry 1). Initially, we investigated the effect of different solvents by testing EtOH, MeOH, and an H_2O/EtOH mixture at various temperatures. The best result was achieved with H_2O/EtOH (3:1) under reflux conditions (Table 1, entry 9).

Then, the reaction was carried out by varying the amount of agar (entries 9–13 in Table 1). The results indicate that 0.15 g of agar is sufficient to carry out the reaction efficiently (Table 1, entry 11). Further increases in the amount of agar in the mentioned reaction did not have any significant effect on product yield or reaction time. Subsequently, the efficiency of starch as another catalyst was tested. This clearly demonstrated that catalysis was solely due to intact agar rather than starch. Therefore, as shown in Table 1, the best results were achieved using 0.15 g of agar as the catalyst in H_2O/EtOH (3:1) under reflux conditions (Table 1, entry 11).

Intrigued by the disappointing results, the model reaction of aldehyde, 2-hydroxy-1,4-naphthoquinone, and malononitrile (molar ratio: 1:1:1) was also studied to establish its optimal conditions (Table 2). In the absence of a catalyst, only trace amounts of the desired product were obtained, even after a long reaction time (entry 1). The reaction was also examined in MeOH and various H_2O/EtOH mixtures. The best result was obtained with H_2O/EtOH (2:1) (Table 4, entry 8). To determine the appropriate amount of a catalyst, the model reaction was investigated with different quantities of agar. The highest yield was obtained using 0.12 g of agar. Increasing the amount of agar did not improve either the yield or the reaction time. As shown in Table 1, the best results were achieved using 0.12 g of the catalyst in refluxed H_2O/EtOH (2:1).

Using these optimized reaction conditions, the scope of the reaction was explored for various substrates. The results of the comprehensive scope are presented in Table 3.

We have not established a mechanism for the formation of 9,9-dimethyl-12-phenyl-9,10-dihydro-8H-benzo[a]xanthen-11(12H)-ones ring systems, but a plausible mechanism in the presence of agar as a catalyst is shown in Figure 14. We have demonstrated that agar forms some kind of micelle-like structures, which can hold molecules and further catalyze reactions, possibly activated by hydrogen bonds. Hydrogen bonding can be formed between protons in OH groups of the agarose polymer in the agar and the substrate, leading to activation during the reaction [3-10].

The first step, condensation of aldehyde 1 and 2-naphthol 2, produces intermediate 4 through dehydration. Then, the activated dimedone 3 reacts with intermediate 4, leading to intermediate 5. In the next step, intermediate 6 is produced by the intermolecular nucleophilic attack of the enol oxygen on the activated carbonyl group, followed by cyclization and proton transfer. Dehydration of 6 yields the final product 7 (Figure 14).

The mechanism for the synthesis of other compounds, such as 14H-dibenzo[a,j]xanthenes and a variety of chromenes prepared in this study, can follow a similar mechanism to the one mentioned above [3, 9, 34, 37, 40, 42].

The optimal conditions for synthesizing xanthene derivatives involved using 0.15 g of agar in a water/ethanol (3:1) mixture at reflux. This method yielded products with up to 95% efficiency. A proposed mechanism suggests that agar forms micelle-like structures, facilitating hydrogen bonding and activation of substrates.

3.2. Molecular docking analysis

Molecular docking analysis is an important tool in drug discovery, helping to circumvent experimental challenges, understand the biological activity networks of drugs, and gain deeper insights into them. The aim of this approach is to predict the best binding pose of a ligand to fit the binding site of a protein and evaluate its binding affinity using a scoring function. Through this strategy, we identified key residues and modes of the synthesized compounds within the active sites of human serum albumin (HSA) and DNA gyrase B. Our results indicate that compounds A2, B9, C2, D12, D'8, E9, and F17 from each class exhibited the lowest binding energy with HSA. The lowest interaction energy or best docking score for the best conformers of these compounds are presented in Table 4. Important interactions, including hydrogen bonds, hydrophobic interactions, and Van der Waals forces, along with the surrounding residues for each compound involved in binding, are listed in Table 5. Schematic illustrations of 2D and 3D interactions of compounds A2, B9, C2, D12, D'8, E9, and F17 with HSA are presented in Figures 2-8.
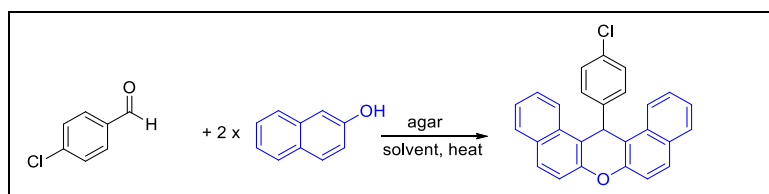
We also conducted docking analyses between chromene-based compounds and DNA gyrase B. This analysis revealed that compounds C2, D12, D'6, E18, and F11 exhibited more favorable interactions with DNA gyrase B. Table 6 lists the types of important interactions and surrounding residues for each compound involved in binding. Figures 11-13 depict hydrogen bonds, hydrophobic interactions, and Van der Waals interactions obtained. Finally, the interaction energies between amino acid residues of the active site of all docking simulations are separately listed in Tables 7-18.

Compounds A2, B9, C2, D12, D'8, E9, and F17 exhibited strong binding affinities with HSA, with binding energies between -8.5 and -9.8 kcal/mol. Key interactions included hydrogen bonds and hydrophobic contacts, critical for their biological activity.

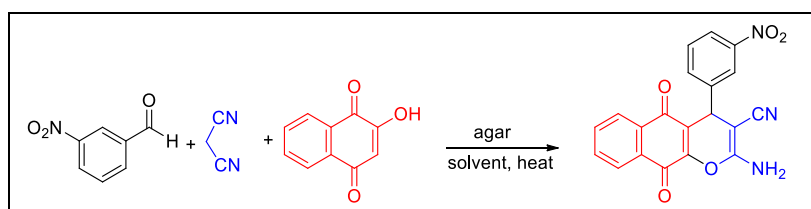## 3.3. *In silico* ADMET properties analysis

ADMET information aids chemists in enhancing the pharmacokinetic features of compounds in rational drug design. These descriptors include log S (aqueous solubility), logP (octanol/water partition coefficient controlling hydrophilicity or lipophilicity of molecules), logBB (blood-brain barrier), logKhsa (serum protein binding), log Kp (skin permeability coefficient), PSA (topological polar surface area), the number of metabolic reactions, and apparent Caco-2 and Madin–Darby canine kidney (MDCK) permeability (the higher the MDCK cell value, the higher the cell permeability) (the higher the value of MDCK cell, the higher the cell permeability), and toxicity risk assessment parameters including mutagenicity, tumorigenicity, irritating effects, and reproductive effects. ADMET properties were calculated and are presented in Table 19. Tissue distribution prediction of a drug is one of the important considerations in drug development. Molecular descriptors such as logP, logBB, and logKhsa have proven to be useful in modeling distribution. Therefore, all the synthesized compounds were expected to be safe toward the central nervous system and to exhibit good distribution. The values of Caco-2 and MDCK for the synthesized compounds good membrane permeability properties. Additionally, log P, aqueous solubility (log S), and topological polar surface area (PSA) descriptors have been proposed for the absorption process. In summary, almost all the synthesized compounds fall within acceptable ranges for the properties analyzed, covering 95% of all known drugs (Table 19).

ADMET analysis showed favorable pharmacokinetic profiles, including high solubility, low toxicity, and good oral bioavailability. These properties underscore the potential of these compounds as drug candidates.

Table 1 Optimization conditions for preparation of 14H-dibenzo[a,j] xanthene derivatives

entry	solvent	T (°C)	cat. (g)	t (min)	yield (%)
1	EtOH	r.t.	-	24 h	Trace
2	EtOH	reflux	0.1	24 h	Trace
3	EtOH	r.t.	0.1	24 h	Trace
4	EtOH	50	0.1	150	39
5	EtOH	reflux	0.1	60	84
6	MeOH	reflux	0.1	45	82
7	H_2O/EtOH(1:1)	reflux	0.1	45	84
8	H_2O/EtOH(2:1)	reflux	0.1	45	87
9	H_2O/EtOH(3:1)	reflux	0.1	45	89
10	H_2O/EtOH(3:1)	reflux	0.05	50	86
11	H_2O/EtOH(3:1)	**reflux**	**0.15**	**40**	**92**
12	H_2O/EtOH(3:1)	reflux	0.2	40	92
13[b]	H_2O/EtOH(3:1)	reflux	0.15	50	90

a isolated yields, b Starch was used as the catalyst.

Table 2 Optimization of the three-component reaction

entry	T (°C)	Solvent	Cat. (g)	t (min)	Yield(%)[a]
1	r.t	EtOH	-	24 h	Trace
2	r.t	EtOH	0.1	24 h	Trace
3	50	EtOH	0.1	120	Trace
4	reflux	EtOH	0.1	45	88
5	reflux	MeOH	0.1	40	81
6	reflux	H_2O-EtOH(1:1)	0.1	45	89
7	reflux	H_2O-EtOH(1:2)	0.1	40	83
8	reflux	H_2O-EtOH(2:1)	0.1	35	93
9	reflux	H_2O-EtOH(3:1)	0.1	35	90
10	reflux	H_2O-EtOH(2:1)	0.05	40	83

| 11 | reflux | H$_2$O-EtOH(2:1) | 0.15 | 35 | 95 |
| 12 | reflux | H$_2$O-EtOH(2:1) | 0.2 | 35 | 95 |

a isolated yields.

Table 3 The scope of the agar-catalyzed reactions includes
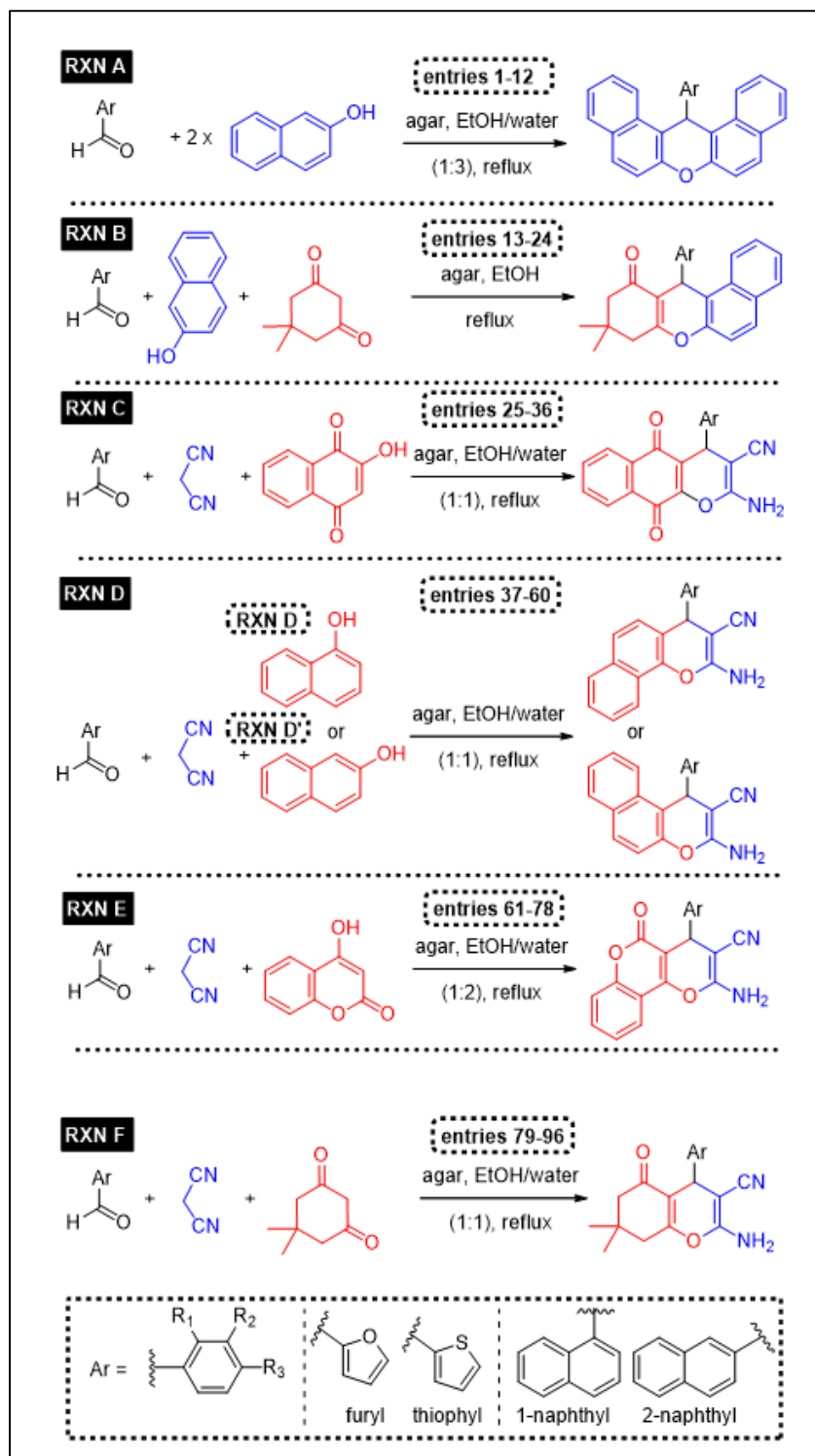
Entry	R_1; R_2; R_3	RXN	t (min)	yield (%)[a]	m.p. /lit. m.p. [Ref] (°C)
1	H; H; H	A1	40	91	185-186/183 [31-35]
2	H; NO$_2$; H	A2	45	90	217-219/213 [31-35]
3	H; H; NO$_2$	A3	45	92	>300/312 [31-35]
4	Cl; H; H	A4	40	93	211-214/213-215 [31-35]
5	H; Cl; H	A5	40	92	169-171/174 [31-35]
6	H; H; Cl	A6	40	90	282-283/286-288 [31-35]
7	H; H; Br	A7	35	91	240/237-238 [31-35]
8	Cl; H; Cl	A8	35	88	229-230/227 [31-35]
9	H; H; Me	A9	65	89	225-227/228 [31-35]
10	OMe; H; H	A10	80	90	256-259/258-259 [31-35]
11	H; H; OMe	A11	75	88	205/206 [31-35]
12	H; H; OH	A12	75	84	144/140 [31-35]
13	H; H; H	B1	50	90	150-153/151-153 [26]
14	H; H; NO$_2$	B2	45	93	174-177/178-180 [26]
15	Cl; H; H	B3	50	92	182-183/179-180 [26]
16	H; H; Cl	B4	45	89	179-180/180-182 [26]
17	Cl; H; Cl	B5	45	88	184/181-182 [26]
18	H; H; F	B6	40	86	193-194/195-197 [5]
19	H; H; Br	B7	55	86	185-188/186-187 [5]
20	furyl	B8	50	89	248/245-246 [6]
21	H; H; Me	B9	80	90	171-172/174-176 [6]
22	H; H; OMe	B10	90	87	201-204/205-206 [26]
23	H; H; OH	B11	90	88	227-228/223-225 [27]
24	H; H : NMe$_2$	B12	85	86	198-199/200-202 [30]
25	H; H; H	C1	35	92	258-229/260-262 [7]
26	H; NO$_2$; H	C2	30	96	239/236-238 [8]
27	Cl; H; H	C3	30	94	251-254/250-252 [8]
28	H; H; Cl	C4	30	96	244/240-242 [7]
29	H; H; F	C5	28	95	243-246/240-242 [8]
30	H; H; Br	C6	30	91	251/252-254 [7]
31	Cl; H; Cl	C7	30	90	250/248-249
32	H; H; CN	C8	35	95	258-259/260-262
33	H; H; Me	C9	55	93	237-239/242-244 [7]
34	H; H; OMe	C10	45	91	243-246/244-246 [8]
35	H; H; OH	C11	45	89	256/255-257 [8]
36	H; OMe; OH	C12	55	87	246-247/243-245 [8]
37	H; H; H	D1	35	94	205-209/207-210 [42]

38	H; NO$_2$; H	D2	30	95	210-211/208-211 [43]
39	H; H; NO$_2$	D3	30	96	231/231-234 [42]
40	Cl; H; H	D4	40	95	234-237/235 [44]
41	H; Cl; H	D5	35	93	228-231/229-230 [38]
42	H; H; Cl	D6	35	94	233-234/229-230 [42]
43	H; H; Br	D7	40	91	233-236/234-235 [45]
44	Cl; H; Cl	D8	30	93	221-223/222-224 [42]
45	H; H; Me	D9	50	89	204-207/205-206 [42]
46	H; H; OMe	D10	60	88	180-183/182-184 [38]
47	H; OMe;OMe	D11	80	82	211/209-210 [7]
48	H; OH; H	D12	55	90	252-254/250-253 [41]
49	furyl	D13	40	88	170/169-172 [43]
50	H; H; H	D'1	30	92	280-281/278-279 [46]
51	H; H; NO$_2$	D'2	35	91	184-187/185-186 [47]
52	Cl; H; H	D'3	35	92	263/265-267 [47]
53	H; H; Cl	D'4	30	94	209-211/210-211 [47]
54	H; H; Br	D'5	35	89	239-242/241-243 [48]
55	Cl; H; Cl	D'6	30	78	238-240/239-240 [47]
56	H; H; Me	D'7	45	89	250-252/253-254 [38]
57	H; OMe; H	D'8	55	86	264/262-263 [47]
58	H; H; OMe	D'9	65	88	191-194/194 [47]
59	H; OMe;OMe	D'10	70	87	142-145/141-143 [49]
60	H; OH; H	D'11	65	89	278-279/280-282 [41]
61	H; H; H	E1	35	94	258-260/257-258 [50]
62	H; H; NO$_2$	E2	30	95	265-268/266-267 [51]
63	H; H; Cl	E3	30	96	261-262/261-262 [50]
64	H; H; F	E4	30	95	260-261/260-262 [7]
65	H; H; Br	E5	30	94	255-258/255-257 [52]
66	Cl; H; Cl	E6	30	89	256-260/261-262 [51]
67	2,6-dichloro	E7	35	92	275-276/274-277 [53]
68	H; H; CN	E8	30	93	285-288/289-290 [54]
69	furyl	E9	25	90	249-252/250-252 [7]
70	thiophyl	E10	45	89	227-230 /228-229 [55]
71	H; H; Me	E11	55	88	253-255/254-255 [56]
72	H; H; OMe	E12	70	88	248-250/247-249 [56]
73	H; OMe; OMe	E13	90	87	263-266/264-266 [4]
74	H; H; OH	E14	70	82	266-269/266-267 [50]
75	H; OMe; OH	E15	70	88	252-253/253-254 [57]

76	H; H; NMe$_2$	E16	85	86	268-269/266-268 [4]
77	H; H; CHO	E17	70	82	>300/>300
78	2-naphthyl	E18	60	76	293-294/295-297 [58]
79	H; H; H	F1	35	94	225-228/226-228 [39]
80	H; NO$_2$; H	F2	30	95	202-203/201-205 [56]
81	H; H; NO$_2$	F3	30	96	176-179/178-180 [59]
82	Cl; H; H	F4	30	95	202-204/200-202 [39]
83	H; H; Cl	F5	30	94	206-207/207-209 [39]
84	H; H; F	F6	30	89	212-215/210-211 [60]
85	H; H; Br	F7	30	91	199-201/197-198 [61]
86	Cl; H; Cl	F8	30	93	114-116/115-117 [62]
87	H; H; CN	F9	25	90	209-212/208-210 [63]
88	H; H; Me	F10	45	89	211-212/209-211 [56]
89	H; H; OMe	F11	55	88	199-201/197-199 [56]
90	H; OMe; OMe	F12	70	82	172-173/170-173 [39]
91	H; H; OH	F13	55	90	205-208/206-208 [61]
92	H; OMe; OH	F14	75	83	235-237/238-240 [45]
93	H; H; NMe$_2$	F15	70	88	209-213/210-212 [64]
94	H; H; CHO	F16	35	89	>300 / >300 [65]
95	1-naphthyl	F17	70	84	215-217/214-215 [60]

Table 4 The docking analysis predicted minimized affinity of the synthesized compounds with HSA and DNA gyrase

Com.	Minimized affinity (kcal/mol) With HSA	Minimized affinity (kcal/mol) With DNA gyrase
A1	-9.78481	-
A2	-11.3093	-
A3	-10.17	-
A4	-9.58038	-
A5	-10.8529	-
A6	-10.0835	-
A7	-10.0306	-
A8	-9.6999	-
A9	-10.1082	-
A10	-9.58878	-
A11	-9.7933	-
A12	-10.0218	-
B1	-9.72867	-

B2	-9.436	-
B3	-9.4241	-
B4	-10.0172	-
B5	-9.72992	-
B6	-9.95261	-
B7	-10.0459	-
B8	-9.32135	-
B9	-10.0976	-
B10	-9.78135	-
B11	-9.98463	-
B12	-9.67155	-
C1	-9.30569	-8.35304
C2	-9.77348	-8.56147
C3	-9.27784	-8.29584
C4	-8.92876	-8.44478
C5	-9.02282	-8.48914
C6	-8.94225	-8.34745
C7	-9.26407	-8.29661
C8	-8.75287	-8.24305
C9	-8.98453	-8.53808
C10	-8.74332	-8.16226
C11	-8.97762	-8.31447
C12	-9.10749	-8.09768
D1	-10.6389	-8.34541
D2	-10.8367	-8.6054
D3	-8.99003	-8.5559
D4	-9.21681	-8.55325
D5	-10.7721	-8.50866
D6	-9.88493	-8.20641
D7	-8.8892	-8.23495
D8	-9.20748	-8.3138
D9	-10.1397	-8.29004
D10	-8.71942	-8.00745
D11	-8.7547	-8.09242
D12	-10.8448	-8.82861
D13	-9.19199	-8.39628
D'1	-8.64308	-7.39831
D'2	-8.52312	-7.45937

D'3	-8.45674	-7.6815
D'4	-8.34768	-7.43615
D'5	-8.38649	-7.43639
D'6	-8.70248	-7.70881
D'7	-8.40649	-7.62069
D'8	-8.75624	-7.5672
D'9	-8.31402	-7.44039
D'10	-8.40166	-7.36421
D'11	-8.68674	-7.69156
E1	-8.18021	-8.75229
E2	-8.92513	-9.05596
E3	-8.40449	-8.69368
E4	-8.36318	-8.8372
E5	-8.42455	-8.56393
E6	-8.8114	-8.80658
E7	-9.35328	-8.80658
E8	-8.29348	-8.60459
E9	-10.3099	-8.69704
E10	-10.0728	-8.62091
E11	-8.41802	-8.70903
E12	-8.23879	-8.69869
E13	-8.36839	-8.59295
E14	-9.34879	-9.04487
E15	-8.47939	-8.9209
E16	-8.31851	-8.55223
E17	-8.40858	-8.59337
E18	-9.85175	-9.39207
F1	-7.98396	-7.29764
F2	-8.05485	-7.13184
F3	-8.27839	-7.33427
F4	-8.04287	-7.0831
F5	-8.18406	-7.15562
F6	-8.1416	-7.4455
F7	-8.20371	-7.4455
F8	-8.22431	-6.63507
F9	-7.91039	-7.53372
F10	-8.25314	-7.32128
F11	-7.99468	-7.86386

F12	-8.06823	-7.8306
F13	-8.11743	-7.76861
F14	-8.19486	-7.50695
F15	-8.23445	-6.35444
F16	-8.09493	-7.48474
F17	-8.89462	-7.72967

Table 5 Amino acid residues involved in the docking results of the synthesized compounds with HSA

Comp.	Hydrophobic interaction	Hydrogen bond	van der waals
A2	ARG114 (Pi-Alkyl, 5.38Å) ARG186 (Pi-Alkyl, 4.53Å) ILE142 (Amide-Pi Stacked 4.65Å) (Alkyl ,4.59Å) (Pi-Alkyl, 4.36Å, 5.49Å) LEU115 (Pi-Alkyl, 4.28Å) TYR161 (Pi-Pi Stacked, 4.59Å, 4.76Å, 5.75Å, 5.98Å) (Pi-Donor, 3.68 Å)	TYR161(-2.48 kcal/mol, 3.1Å) (-1.06 kcal/mol, 3.38Å) LEU185(-2.5 kcal/mol, 3.08Å)	ARG145-GLY189-HIS146-LEU182-LYS190-PHE157-VAL116
B9	ARG145 (Alkyl, 4.49Å) ARG185 (Pi-Sigma, 3.44Å, 3.84Å) HIS146 (Pi-Alkyl, 4.97Å) ILE142 (Alkyl ,4.24Å) (Pi-Alkyl, 5.36Å) LEU115 (Pi-Alkyl, 5.24Å) LEU154 (Alkyl, 4.84Å) PHE157 (Pi-Alkyl, 4.05Å, 4.45Å) TYR161 (Pi-Alkyl, 5.21Å, 5.38Å)	TYR161 (-1.79 kcal/mol, 3.24Å)	GLY189-LEU185-LYS190
C2	ILE142 (Pi-Alkyl, 4.11Å, 4.75Å) LEU182 (Pi-Alkyl, 5.07Å) TYR161 (Pi-Pi Stacked, 4.00Å, 4.39Å) (Pi-Donor, 3.21Å) (Pi-Pi T-Shaped, 5.15Å)	TYR161 (-2.5 kcal/mol, 2.69Å) ARG117 (C-H, 3.61Å)	ALA158-ARE186-PHE157-PRO118-TYR138
D12	ILE142 (Pi-Alkyl, 4.18Å, 4.37Å) LEU182 (Pi-Alkyl, 4.99Å) MET123 (Pi-Sulfur, 5.99Å) TYR161 (Pi-Pi Stacked, 4.29Å, 4.57Å) (Pi-Donor, 3.75Å, 3.83Å)	TYR161 (-2.5 kcal/mol, 2.97Å)	ALA158-ARE186-PHE157-PHE165-TYR138

	(Pi-Pi T-Shaped, 4.78Å)		
D·8	ILE142 (Pi-Sigma, 3.52Å) (Pi-Alkyl, 4.2Å) LEU182 (Pi-Alkyl, 4.98Å) TYR138 (Pi-Sigma, 3.78Å) TYR161 (Pi-Pi Stacked, 4.22Å, 5.01Å) (Pi-Donor, 3.13Å, 3.57Å, 3.71Å) (Pi-Pi T-Shaped, 5.13Å)	TYR161	ARG186-PHE165
E9	ARG186 (Pi-Alkyl, 5.36Å) LEU139 (Amide-Pi Stacked, 4.55Å) LEU182 (Pi-Alkyl, 4.55Å) TYR138 (Pi-Pi Stacked, 4.74Å, 5.71Å) TYR161 (Pi-Pi Stacked, 3.92Å, 4.00Å) (Pi-Donor, 3.33Å, 3.94Å) (Pi-Pi T-Shaped, 4.90Å)	ARG117 (C-H) TYR161 (-1.48 kcal/mol, 3.3Å)	ALA158-ARG117-ILE142-LEU135-LEU139-PHE165-PRO118
F17	ARG117 (Alkyl, 4.74Å) ARG186 (Pi-Alkyl, 5.16Å) LEU115 (Pi-Alkyl, 5.10Å) LEU182 (Alkyl, 3.58Å, 4.63Å, 4.94Å) LYS190 (Pi-Alkyl, 4.64Å) TYR161 (Pi-Alkyl, 4.85Å)	ARG117 (-2.13 kcal/mol, 3.07Å) (-0.93 kcal/mol, 3.34Å) TYR161 (-2.42 kcal/mol, 2.97Å)	GLY189-PHE165

Table 6 Amino acid residues involved in the docking results of the synthesized chromenes with DNA gyrase

Comp.	Hydrophobic interaction	Hydrogen bond	van der waals
C2	ILE78 (Pi-Sigma, 3.80Å) ASP49 (Amide-Pi Stacked, 5.20Å) (Pi-Donor, 3.75Å, 4.19Å) ALA47 (Pi-Alkyl, 4.67Å)	ARG76 (-2.06 kcal/mol, 3.18Å) (-1.1 kcal/mol, 3.37Å) ASN46	ALA53-GLU50-THR165-VAL43
D12	ALA47 (Pi-Alkyl, 4.68Å) ASN46 (Amide-Pi Stacked, 4.26Å, 4.66Å) ILE78 (Pi-Alkyl, 5.05Å) VAL43 (Pi-Alkyl, 5.43Å) VAL167 (Pi-Alkyl, 5.36Å)	ASP49 (-2.5 kcal/mol, 3.09Å) (-0.55 kcal/mol, 3.46Å) ASN46 (-1.63 kcal/mol, 3.27Å)	GLU50-THR165-VAL71
D,6	ASP73 (Pi-Anion 4.98Å) GLU50 (Pi-Anion 3.57Å) ILE78 (Pi-Alkyl, 4.66Å, 5.17Å) ILE90 (Alkyl 4.14Å)	-	ALA47-ARG76-THR165
E18	ASN46 (Pi-Sigma, 3.80Å) (Pi-Donor, 3.29Å, 4.04Å) ILE78 (Pi-Sigma, 3.96Å)	ASN46 (-2.23 kcal/mol, 3.15Å) ILE78-PRO79 (C-H)	ASP49-MET91-THR165-VAL43

	(Pi-SigmaAlkyl, 4.91Å) ILE90 (Pi-Alkyl, 5.38Å) VAL120 (Pi-Alkyl, 5.20Å)		
F11	ARG78 (Donor-Donor 1.99Å) GLU50 (Pi-Anion 4.92Å) ILE78 (Pi-Alkyl, 4.53Å) ILE90 (Pi-Alkyl, 4.48Å, 5.11Å, 5.41Å)	GLU50 (-2.5 kcal/mol, 3.05Å)	ALA47-THR165

Table 7 Interaction energy between the product A2 and responsive amino acid residues of HSA in molecular docking

Amino acid residues	Interaction energy kJ mol^{-1}
Arg114	-7.93913
Arg117	-3.89802
Arg145	-2.75295
Arg186	-10.2557
Asp187	-0.42931
Gly189	-4.50678
His146	-2.2454
Ile142	-11.8516
Leu115	-27.1551
Leu154	-0.32485
Leu182	-0.36876
Leu185	-7.52471
Lys190	-5.1365
Phe157	-5.37404
Tyr138	-13.109
Tyr161	-21.9612
Val116	-8.27258

Table 8 Interaction energy between the product B8 and the amino acid residues involved in the docking results with HSA

Amino acid residues	Interaction energy kJ mol^{-1}
Arg114	-6.05091
Arg117	-4.70494
Arg145	-10.4665
Arg186	-15.5194
Gly189	-5.71542
His146	-6.94177
Ile142	-13.8995

Leu112	-0.4538
Leu115	-11.4222
Leu154	-1.35909
Leu182	-1.16163
Leu185	-2.24035
Lys190	-9.50379
Phe149	-0.87408
Phe157	-6.72687
Pro113	-1.72116
Tyr161	-12.4237
Val116	-1.17344

Table 9 Interaction energy between the product C2 and the amino acid residues involved in the docking results with HSA.

Amino acid residues	Interaction energy kJ mol^{-1}
Ala158	-2.87786
Arg117	-11.1463
Arg186	-2.13683
Ile142	-15.6857
Leu115	-8.5165
Leu139	-4.48663
Leu154	-2.56345
Leu182	-7.51093
Leu185	-0.31035
Met123	-2.51438
Phe157	-5.00527
Pro118	-2.28535
Tyr138	-17.7093
Tyr161	-31.717
Val116	-6.56234

Table 10 Interaction energy between the product D12 and the amino acid residues involved in the docking results with HSA

Amino acid residues	Interaction energy kJ mol⁻¹
Ala158	-2.44475
Arg117	-4.46988
Arg186	-1.97417
Ile142	-17.008
Leu115	-6.04048
Leu139	-5.09943
Leu154	-5.2944
Leu182	-9.55833
Met123	-0.5533
Phe157	-6.32859
Phe165	-1.1083
Tyr138	-15.9356
Tyr161	-35.3328
Val116	-2.34129

Table 11 Interaction energy between the product D᾽8 and the amino acid residues involved in the docking results with HSA

Amino acid residues	Interaction energy kJ mol⁻¹
Arg117	-6.2529
Arg186	-7.20766
Gly189	-0.32173
Ile142	-14.649
Leu115	-6.49889
Leu139	-2.32908
Leu182	-9.06903
Leu185	-1.62938
Lys190	-0.36636
Met123	-1.33225
Phe134	-0.34788
Phe157	-0.49797
Phe165	-1.36903
Tyr138	-14.6832
Tyr161	-27.2244
Val116	-3.33134

Table 12 Interaction energy between the product E9 and the amino acid residues involved in the docking results with HSA

Amino acid residues	Interaction energy kJ mol^{-1}
Ala158	-2.79595
Arg117	-7.09529
Arg186	-2.07847
Asp183	-0.41761
Ile142	-4.74807
Leu115	-1.37065
Leu135	-6.28835
Leu139	-6.6999
Leu182	-9.67823
Leu185	-0.37246
Met123	-3.80449
Phe134	-2.57263
Phe165	-4.42098
Pro118	-2.31988
Tyr138	-40.2546
Tyr161	-39.4974
Val116	-2.54773

Table 13 Interaction energy between the product F17 and the amino acid residues involved in the docking results with HSA

Amino acid residues	Interaction energy kJ mol-1
Arg117	-20.2171
Arg186	-13.3058
Asp187	-0.41345
Gly189	-3.18046
His146	-2.29373
Ile142	-4.82654
Leu115	-6.66167
Leu182	-7.7041
Leu185	-1.19566
Lys190	-11.0917
Met123	-0.42166
Tyr138	-1.65619
Tyr161	-11.0529
Val116	-5.75457

Table 14 Interaction energy between the product C2 and the amino acid residues involved in the docking results with DNA gyrase B

Amino acid residues	Interaction energy / kJ mol^{-1}
Ala47	-8.62101
Ala53	-0.49162
Arg76	-2.42285
Asn46	-33.681
Asp49	-10.9315
Asp73	-4.51304
Glu50	-12.626
Ile78	-17.628
Ile90	-2.82607
Met91	-2.0592
Pro79	-1.73671
Thr165	-9.14078
Val43	-6.37349
Val71	-1.79547
Val120	-3.31464
Val167	-2.4408

Table 15 Interaction energy between the product D12 and the amino acid residues involved in the docking results with DNA gyrase B

Amino acid residues	Interaction energy / kJ mol^{-1}
Ala47	-8.87917
Arg76	-0.44069
Asn46	-34.0831
Asp45	-0.34208
Asp49	-10.0477
Asp73	-3.76889
Glu50	-10.5584
Ile78	-17.2281
Ile90	-3.23943
Met91	-1.7335
Met166	-0.42369
Pro79	-0.56476
Thr165	-13.5368

Val43	-5.54579
Val71	-3.32711
Val120	-4.48978
Val167	-3.91164

Table 16 Interaction energy between the product D,6 and the amino acid residues involved in the docking results with DNA gyrase B

Amino acid residues	Interaction energy / kJ mol^{-1}
Ala47	-1.67424
Ala96	-0.54095
Arg76	-7.57986
Arg136	-0.57447
Asn46	-15.0012
Asp45	-0.3238
Asp49	-8.70856
Asp73	-2.01453
Glu50	-22.1911
Gly77	-6.17022
Ile78	-11.8257
Ile90	-4.18413
Pro79	-2.56698
Thr165	-3.7273

Table 17 Interaction energy between the product E18 and the amino acid residues involved in the docking results with DNA gyrase B

Amino acid residues	Interaction energy / kJ mol^{-1}
Ala47	-5.30714
Ala96	-1.42602
Asn46	-31.3951
Asp45	-0.35928
Asp49	-4.23265
Asp73	-2.71304
Glu50	-7.46947
Gly77	-1.41933
Gly119	-0.48542
Ile78	-18.7989
Ile90	-9.77607

Met91	-1.18638
Pro79	-3.73884
Thr165	-7.61996
Val43	-2.64314
Val120	-3.44765
Val167	-2.09999

Table 18 Interaction energy between the product F11 and the amino acid residues involved in the docking results with DNA gyrase B

Amino acid residues	Interaction energy / kJ mol^{-1}
Ala47	-4.56085
Ala96	-0.78183
Arg76	-4.46099
Asn46	-10.5261
Asp49	-1.03451
Asp73	-1.15559
Glu50	-17.2859
Gly77	-5.87892
Ile78	-17.1912
Ile90	-7.86263
Pro79	-3.84262
Thr165	-6.83262
Val43	-0.4387

Table 19 Prediction of ADME properties of the retrieved hit compounds and toxicity risk assessment using Qikprop

Descriptors	A2	B9	C2	D12	D·6	Stand. Range[a]
logS(aqueous solubility)	-7.3	-7.3	-3.63	-5.24	-6.48	-6.5 to 0.5
logP for octanol/water	6.02	5.89	0.821	2.716	4.22	-2.0 to 6.5
log BB for brain/blood	-0.39	0.303	-1.36	-1.19	-0.276	-3.0 to 1.2
logKhsa (serum protein binding)	1.5	1.348	-0.285	0.275	0.623	-1.5 to 1.5
logKp (Skin-permeability coefficient)	-1.26	-0.91	-4.296	-3.111	-2.33	-8.0 to -1.0, Kp in cm/h
PSA(topological polar surface area)	55.05	26.3	139	79.27	59.04	≤140 is great
No. of metabolic reaction	3	4	3	3	1	1 to 8
Apparent Caco-2 permeability (nm/s)	1277	5478	84.8	232.4	879.65	<25 poor, >500 great
Apparent MDCK permeability (nm/s)	644	3110	34.37	102.8	1875.3	<25 poor, >500 great
mutagenicity	high	high	none	low	high	-
tumorigenicity	high	high	none	low	high	-

| irritating effects | none | none | none | none | none | - |
| reproductive effects | none | none | none | none | none | - |

Continued Table 9

Descriptors	D·8	E9	E18	F11	F17	Stand. Range[a]
logS(aqueous solubility)	-5.62	-4.26	-5.98	-5.37	-5.72	-6.5 to 0.5
logP for octanol/water	3.48	1.603	3.23	2.48	3.14	-2.0 to 6.5
log BB for brain/blood	-0.673	-0.97	-1.102	-0.974	-0.773	-3.0 to 1.2
logKhsa (serum protein binding)	0.463	-0.127	0.393	0.237	0.48	-1.5 to 1.5
logKp (Skin-permeability coefficient)	-2.182	-3.161	-2.821	-3.52	-3.06	-8.0 to -1.0, Kp in cm/h
PSA(topological polar surface area)	68.24	99.48	85.34	85.34	76.11	≤140 is great
No. of metabolic reaction	3	2	1	4	3	1 to 8
Apparent Caco-2 permeability (nm/s)	781.82	287.17	286.51	394.91	492.68	<25 poor, >500 great
Apparent MDCK permeability (nm/s)	379.15	128.42	128.11	181.22	230.17	<25 poor, >500 great
mutagenicity	high	none	none	none	none	-
tumorigenicity	high	none	none	none	high	-
irritating effects	none	none	none	low	none	-
reproductive effects	none	none	none	none	none	-
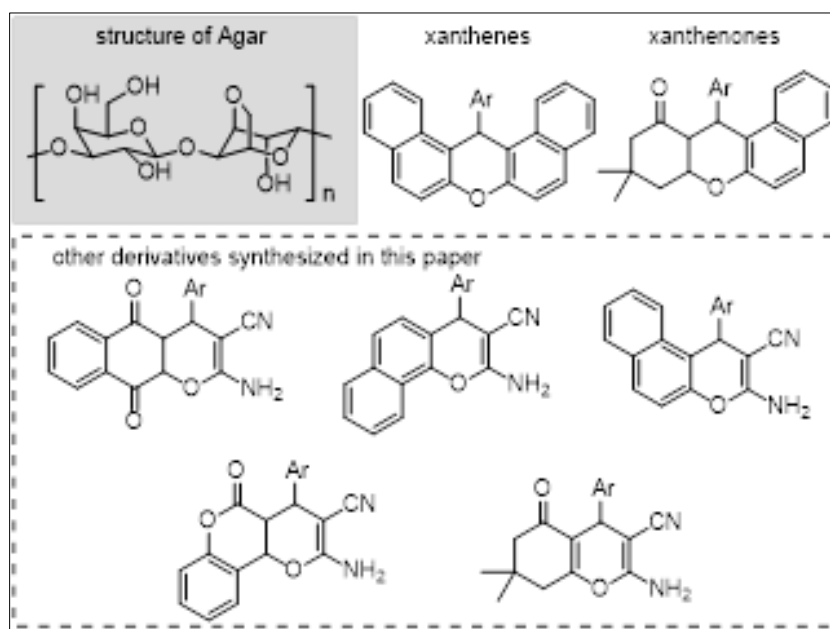
Figure 1 The structure of agar and the synthesized derivatives
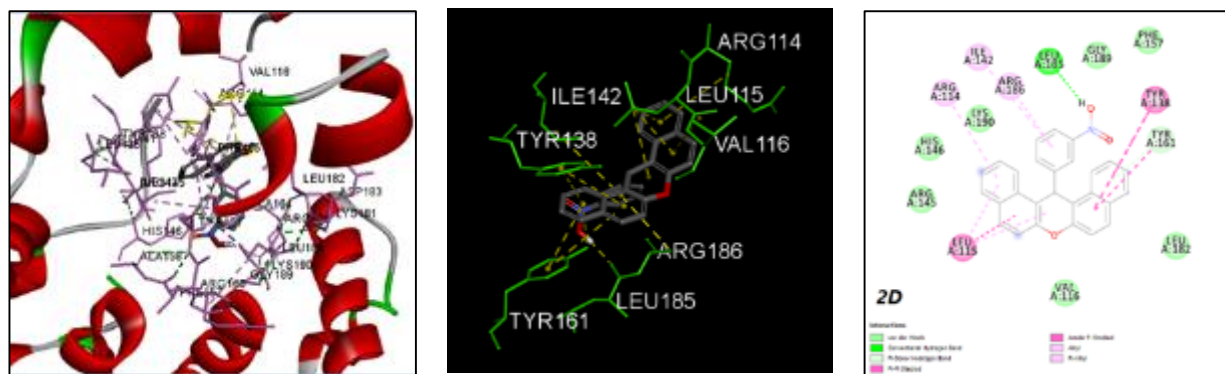
Figure 2 3D and 2D binding mode of compound A2 with HAS
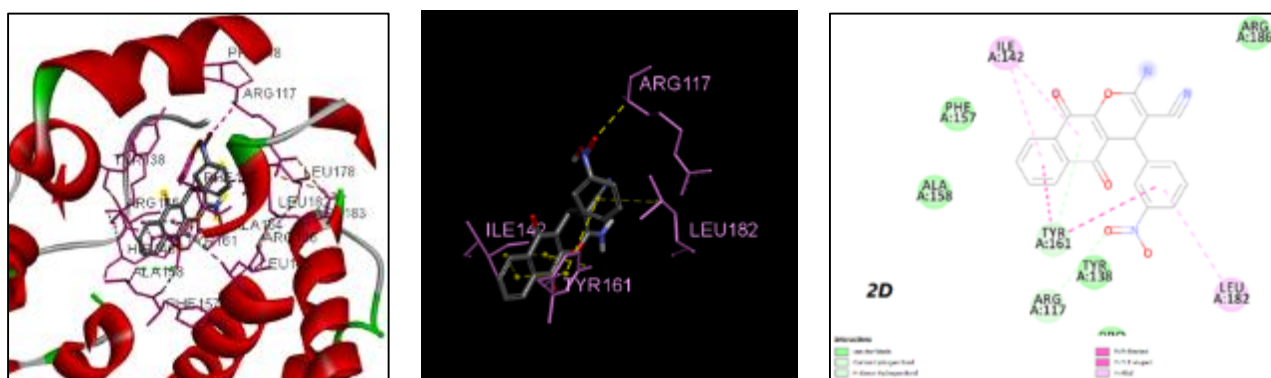
Figure 3 3D and 2D binding mode of compound C2 with HAS
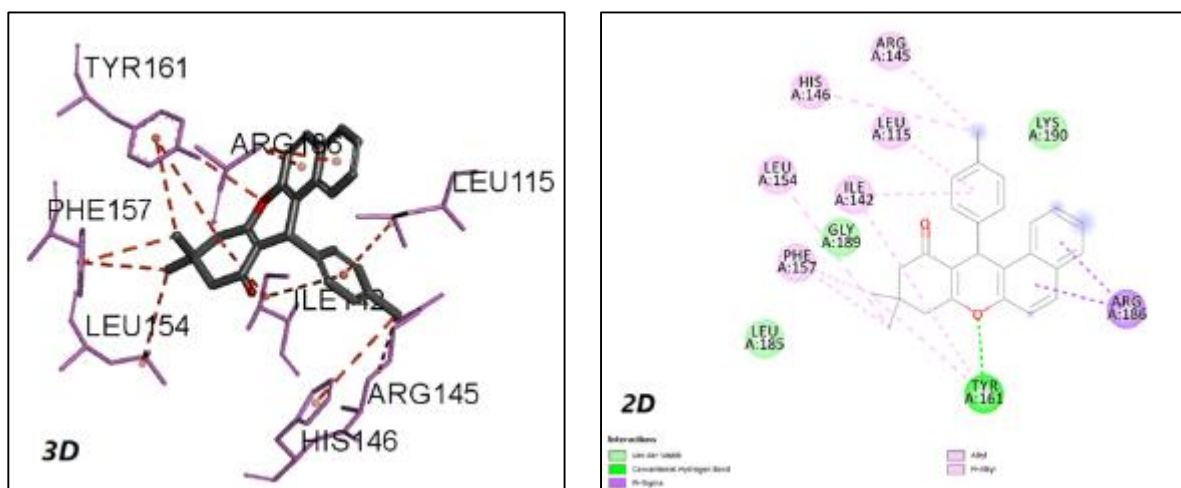
Figure 4 3D and 2D binding mode of compound B9 with HAS
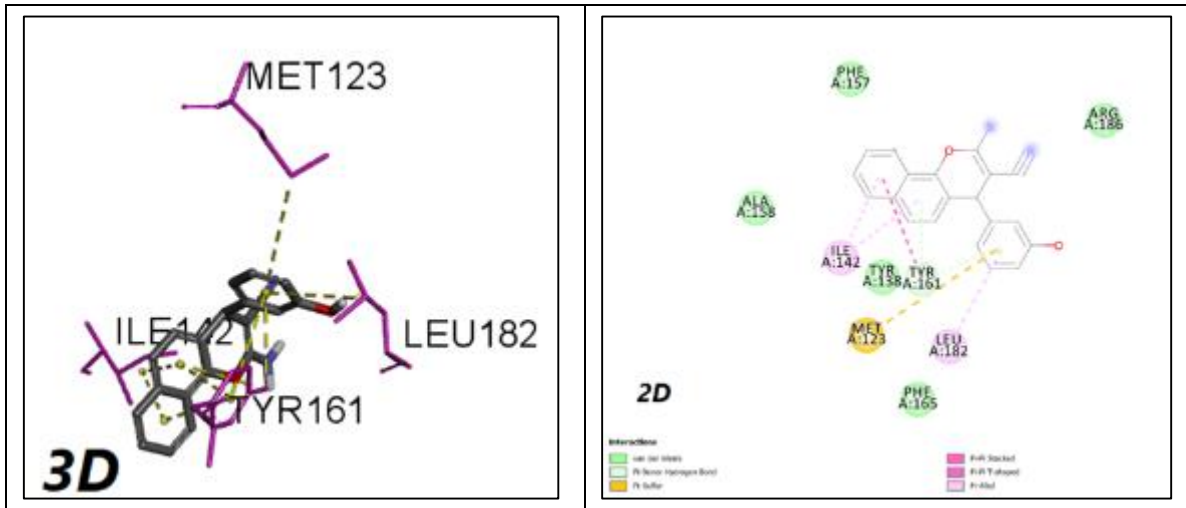
Figure 5 3D and 2D binding mode of compound D12 with HSA
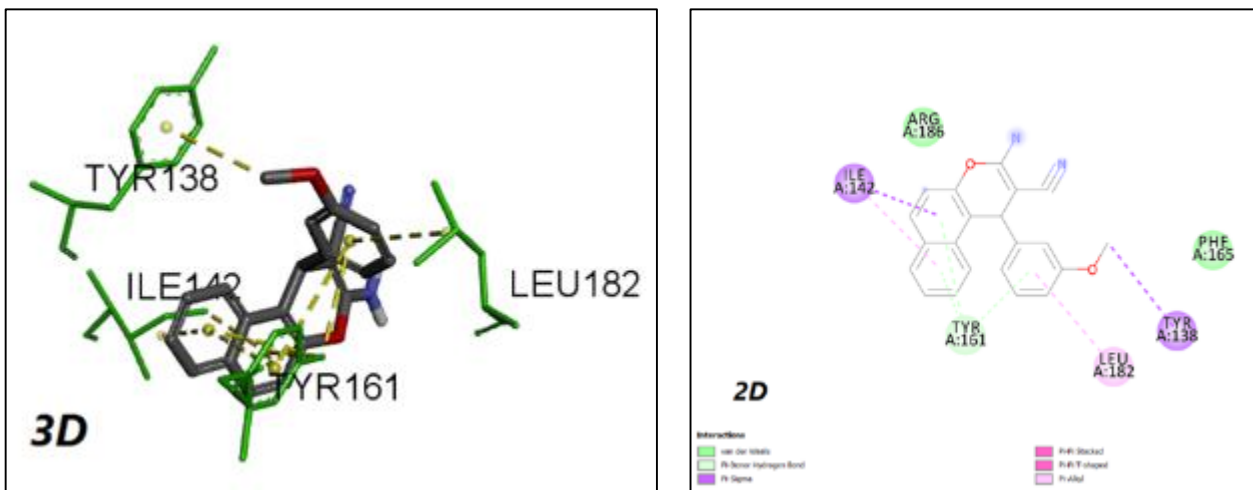
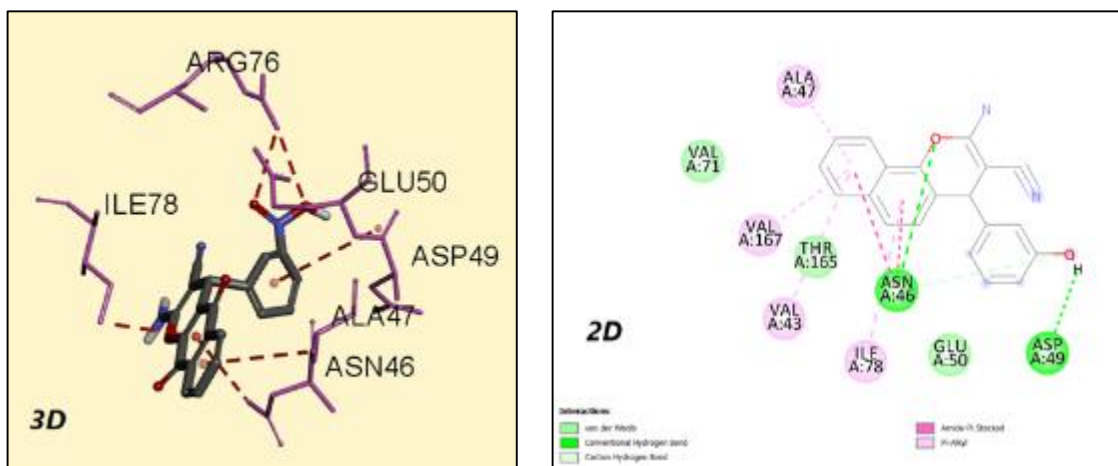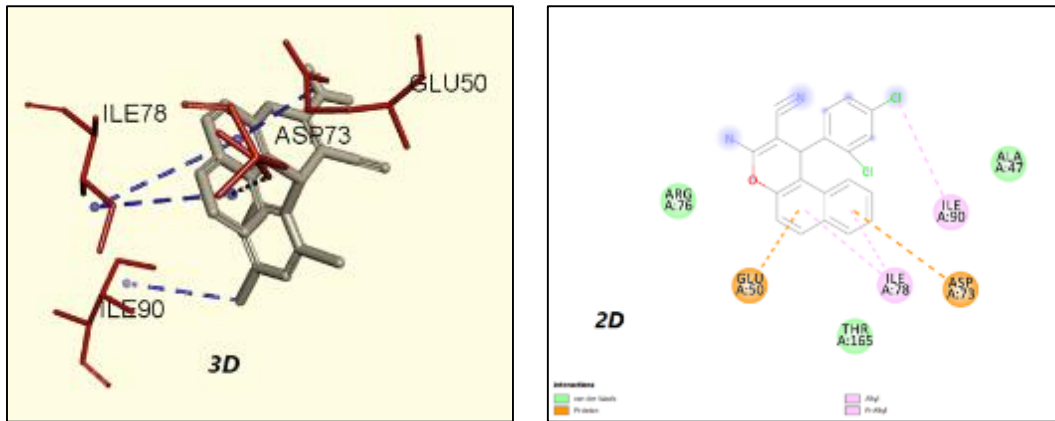**Figure 6** 3D and 2D binding mode of compound D,8 with HSA
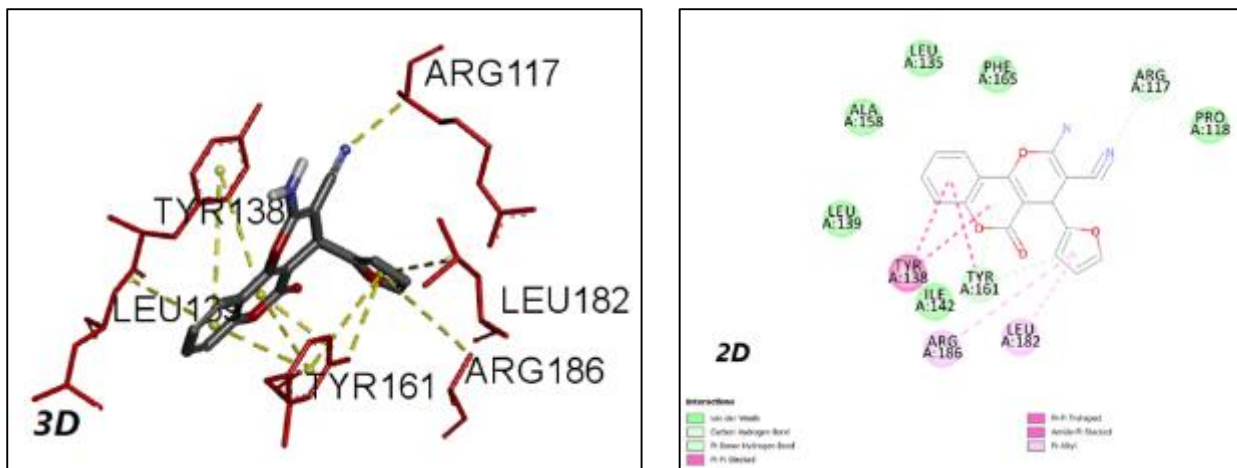
Figure 7 3D and 2D binding mode of compound E9 with HAS
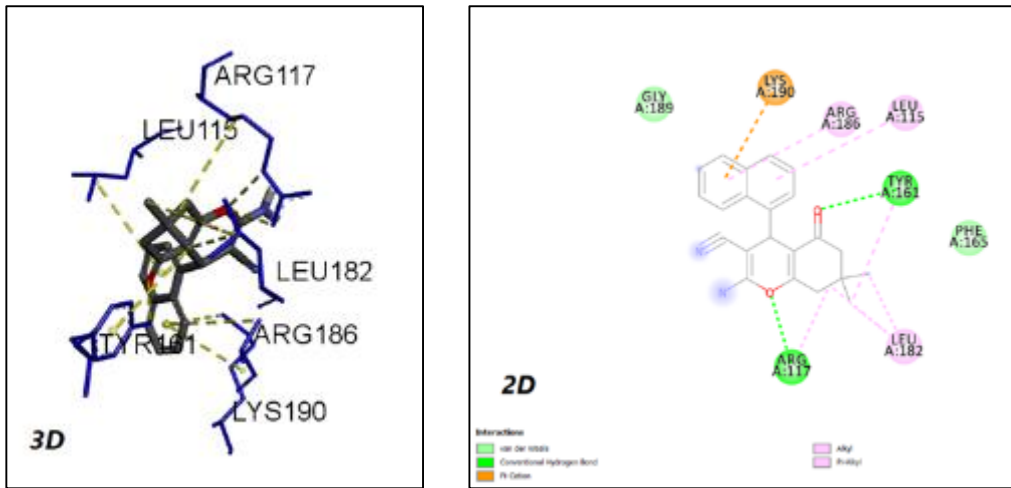
Figure 8 3D and 2D binding mode of compound F17 with HSA
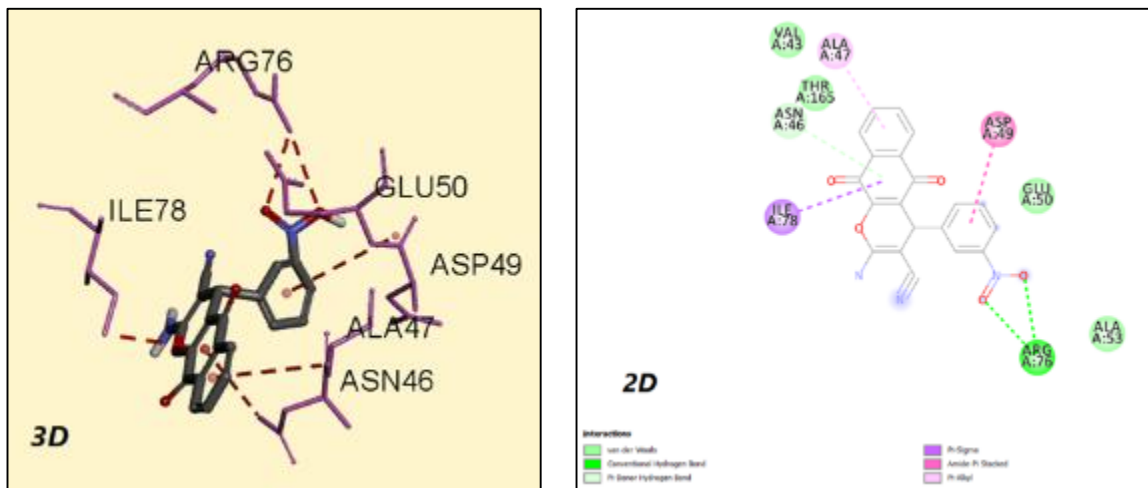
Figure 9 3D and 2D binding mode of compound C2 with DNA gyrase

Figure 10 3D and 2D binding mode of compound D12 with DNA gyrase

Figure 11 3D and 2D binding mode of compound D.6 with DNA gyrase
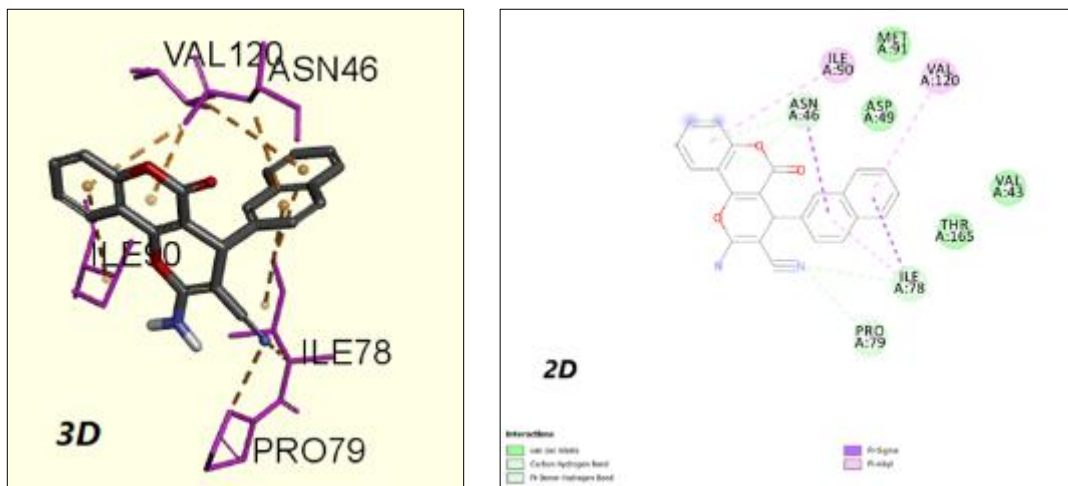
Figure 12 3D and 2D binding mode of compound E18 with DNA gyrase
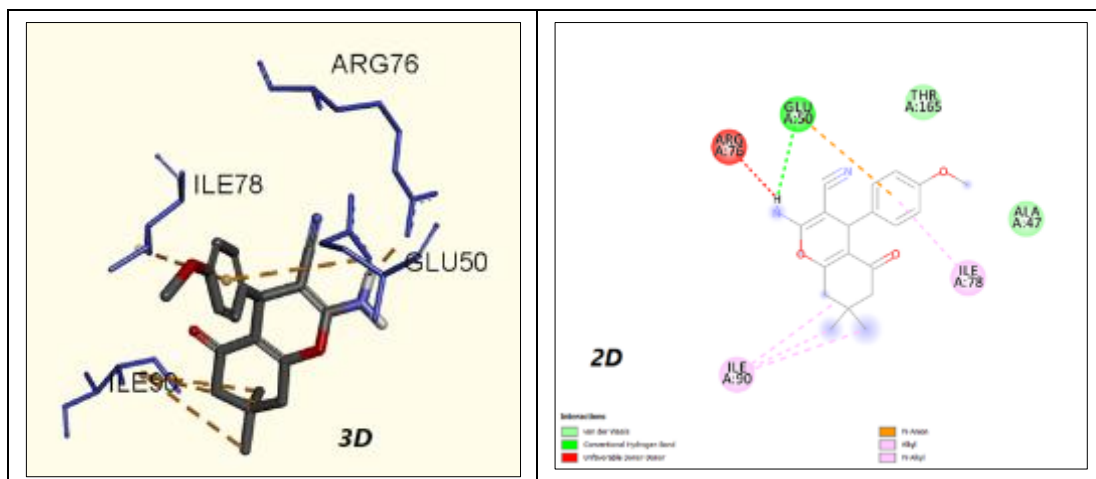
Figure 13 3D and 2D binding mode of compound F11 with DNA gyrase
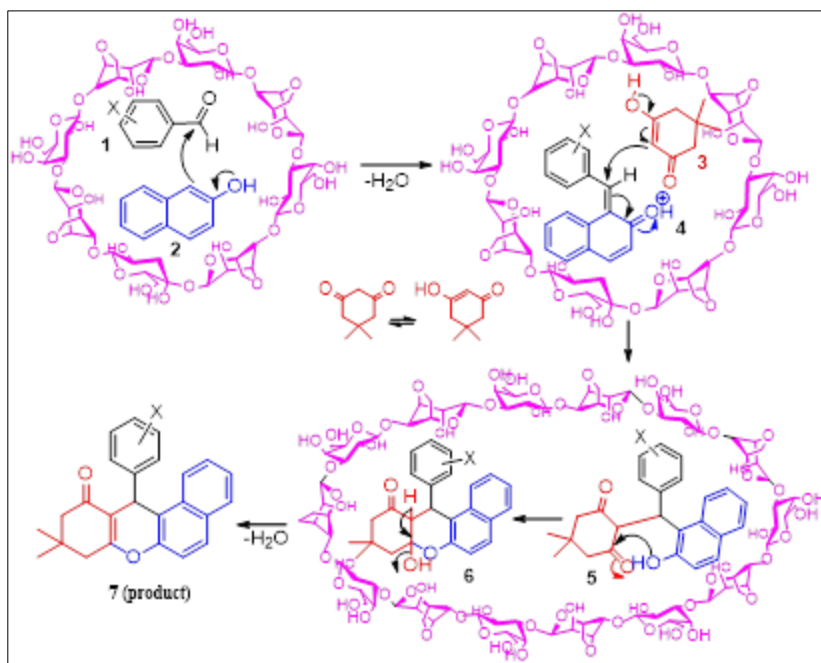
Figure 14 A plausible mechanism for the formation of 9,9-dimethyl-12-phenyl-9,10-dihydro-8H-benzo[a]xanthen-11(12H)-one

4. Conclusions

The present protocol has several significant advantages:

- The natural catalyst is biodegradable, nontoxic, environmentally friendly, and inexpensive;
- High yields and short reaction times;
- Clean reaction conditions; and
- A simple work-up procedure.

These advantages together make a useful and instrumental alternative to the existing methodologies.

In this study, we have showcased the potential of utilizing the natural catalyst agar for synthesizing biologically significant compounds such as xanthene and chromene derivatives, presenting a sustainable and efficient green synthesis approach. Our findings highlight the remarkable anticancer and antibacterial activities exhibited by these compounds, suggesting their potential therapeutic relevance. Furthermore, molecular docking analyses shed light on the intricate molecular interactions of these compounds with key proteins such as human serum albumin (HSA) and DNA gyrase, underscoring their promising potential for drug delivery and antibacterial properties. Additionally, our ADMET analysis underscores the favorable pharmacokinetic properties and drug-likeness of these synthesized compounds, suggesting their suitability for drug development. Pharmacokinetic properties, toxicity risk assessment, and drug-likeness of the synthesized compounds were computed, and most of them were within acceptable ranges. In essence, this study underscores the potential of green synthesis strategies in the development of novel therapeutics, presenting a pathway towards sustainable drug discovery and development.

This study demonstrates a green, efficient synthesis method for xanthene and chromene derivatives using agar as a catalyst. The synthesized compounds exhibit promising anticancer and antibacterial activities, supported by molecular docking and ADMET studies. This environmentally friendly approach paves the way for developing new therapeutic agents with significant clinical potential.

Compliance with ethical standards

Disclosure of conflict of interest

No conflict of interest to be disclosed.

References

[1] F.F. ABDEL-LATIF, Heterocycles Synthesis Through Reactions of Nucleophiles with Acrylonitriles. Part 11. A Convenient One-Pot Synthesis of 4H-Chromenes, ChemInform 21(42) (1990) no-no.

[2] M. Ahmad, T.A. King, D.-K. Ko, B.H. Cha, J. Lee, Performance and photostability of xanthene and pyrromethene laser dyes in sol-gel phases, Journal of Physics D: Applied Physics 35(13) (2002) 1473.

[3] a) A. Moradi, R. Heydari, M.T. Maghsoodlou, Agar: a novel, efficient, and biodegradable catalyst for the one-pot three-component and green synthesis of 2, 3-dihydroquinazolin-4 (1H)-one, 4H-pyrimidobenzothiazole and 2-aminobenzothiazolomethylnaphthol derivatives, Research on Chemical Intermediates 41(10) (2015) 7377-7391. b) A. Kakeshpour, A. Moradi, F. Moradi, Green Synthesis of Xanthenes: Utilizing Sulfonated Fructose as an Efficient and Eco-friendly Catalyst, Journal of Pharmaceutical Research International 36(7) (2024) 59-78.

[4] P. Sahu, RSC Adv., 2013, 3, 9854;(d) PK Sahu, PK Sahu, SK Gupta and DD Agarwal, Ind. Eng. Chem. Res 53 (2014) 2085.

[5] S. Shinde, G. Rashinkar, R. Salunkhe, DABCO entrapped in agar-agar: A heterogeneous gelly catalyst for multi-component synthesis of 2-amino-4H-chromenes, Journal of Molecular Liquids 178 (2013) 122-126.

[6] N. Hazeri, M.T. Maghsoodlou, F. Mir, M. Kangani, H. Saravani, E. Molashahi, An efficient one-pot three-component synthesis of tetrahydrobenzo [b] pyran and 3, 4-dihydropyrano [c] chromene derivatives using starch solution as catalyst, Chinese Journal of Catalysis 35(3) (2014) 391-395.

[7] A. Kakeshpour, A. Moradi, M.T. maghsoodlou, F. Moradi, A Novel Efficient and Biodegradable Natural Catalyst and Bio Based Solvents for the Green One Pot Three Component Synthesis of Tetrahydrobenzo[B]pyran and 3,4-Dihydropyrano[C]chromenes, Journal of Pharmaceutical Research International 36(7) (2024) 13-26.

[8] R.-Z. Wang, L.-F. Zhang, Z.-S. Cui, Iodine-catalyzed synthesis of 12-aryl-8, 9, 10, 12-tetrahydro-benzo [a] xanthen-11-one derivatives via multicomponent reaction, Synthetic Communications® 39(12) (2009) 2101-2107.

[9] a) J.M. Khurana, D. Magoo, pTSA-catalyzed one-pot synthesis of 12-aryl-8, 9, 10, 12-tetrahydrobenzo [a] xanthen-11-ones in ionic liquid and neat conditions, Tetrahedron Letters 50(33) (2009) 4777-4780 b) J.M. Khurana, B. Nand, P. Saluja, DBU: a highly efficient catalyst for one-pot synthesis of substituted 3, 4-dihydropyrano [3, 2-c] chromenes, dihydropyrano [4, 3-b] pyranes, 2-amino-4H-benzo [h] chromenes and 2-amino-4H benzo [g] chromenes in aqueous medium, Tetrahedron 66(30) (2010) 5637-5641.

[10] Y. Yu, H. Guo, X. Li, An improved procedure for the three-component synthesis of benzo [g] chromene derivatives using basic ionic liquid, Journal of Heterocyclic Chemistry 48(6) (2011) 1264-1268.

[11] G. Trinchieri, Cancer immunity: lessons from infectious diseases, The Journal of infectious diseases 212(suppl_1) (2015) S67-S73.

[12] R. Devakaram, D.S. Black, V. Choomuenwai, R.A. Davis, N. Kumar, Synthesis and antiplasmodial evaluation of novel chromeno [2, 3-b] chromene derivatives, Bioorganic & medicinal chemistry 20(4) (2012) 1527-1534.

[13] Q. Ren, W.Y. Siau, Z. Du, K. Zhang, J. Wang, Expeditious assembly of a 2-amino-4H-chromene skeleton by using an enantioselective mannich intramolecular ring cyclization–tautomerization cascade sequence, Chemistry–A European Journal 17(28) (2011) 7781-7785.

[14] K. Niknam, N. Borazjani, R. Rashidian, A. Jamali, Silica-bonded N-propylpiperazine sodium n-propionate as recyclable catalyst for synthesis of 4H-pyran derivatives, Chinese Journal of Catalysis 34(12) (2013) 2245-2254.

[15] A. Kumar, M.K. Gupta, M. Kumar, L-Proline catalysed multicomponent synthesis of 3-amino alkylated indoles via a Mannich-type reaction under solvent-free conditions, Green Chemistry 14(2) (2012) 290-295.

[16] J.H. Clark, Green chemistry: today (and tomorrow), Green Chemistry 8(1) (2006) 17-21.

[17] K. Parida, S. Mallick, P. Sahoo, S. Rana, A facile method for synthesis of amine-functionalized mesoporous zirconia and its catalytic evaluation in Knoevenagel condensation, Applied Catalysis A: General 381(1-2) (2010) 226-232.

[18] M. Costa, F. Proença, 2-Aryl-1, 9-dihydrochromeno [3, 2-d] imidazoles: a facile synthesis from salicylaldehydes and arylideneaminoacetonitrile, Tetrahedron 67(10) (2011) 1799-1804.

[19] J.P. POUPELIN, G. Saint-Ruf, O. Foussard-Blanpin, G. Narcisse, G. Uchida-Ernouf, R. Lacroix, Synthesis and antiinflammatory properties of bis (2-hydroxy-1-naphthyl) methane derivatives. I. Monosubstituted derivatives, Chemischer Informationsdienst 9(25) (1978) no-no.

[20] R. Lambert, J. Martin, J. Merrett, K. Parkes, G. Thomas, PCT Int. Appl. WO 9706178, 1997, Chem. Abstr, 1997, p. 212377y.

[21] R.-M. Ion, A. Planner, K. Wiktorowicz, D. Frackowiak, The incorporation of various porphyrins into blood cells measured via flow cytometry, absorption and emission spectroscopy, ACTA BIOCHIMICA POLONICA-ENGLISH EDITION- 45 (1998) 833-845.

[22] A. Banerjee, A. Mukherjee, Chemical aspects of santalin as a histological stain, Stain technology 56(2) (1981) 83-85.

[23] C.G. Knight, T. Stephens, Xanthene-dye-labelled phosphatidylethanolamines as probes of interfacial pH. Studies in phospholipid vesicles, Biochemical Journal 258(3) (1989) 683-687.

[24] J. Poupaert, P. Carato, E. Colacino, 2 (3H)-benzoxazolone and bioisosters as "privileged scaffold" in the design of pharmacological probes, Current medicinal chemistry 12(7) (2005) 877-885.

[25] D.J. Triggle, 1, 4-Dihydropyridines as calcium channel ligands and privileged structures, Cellular and molecular neurobiology 23(3) (2003) 293-303.

[26] S. Mohr, Chirigos. MA, Fuhrman, FS, and Pryor, JW Pyran Copolymer as an Effective Adjuvant to Chemotherapy against a Murine Leukemia and Solid Tumor, Cancer Res 35 (1975) 3750-3754.

[27] M. Kidwai, S. Saxena, M.K.R. Khan, S.S. Thukral, Aqua mediated synthesis of substituted 2-amino-4H-chromenes and in vitro study as antibacterial agents, Bioorganic & Medicinal Chemistry Letters 15(19) (2005) 4295-4298.

[28] A. Kumar, S. Sharma, R.A. Maurya, J. Sarkar, Diversity oriented synthesis of benzoxanthene and benzochromene libraries via one-pot, three-component reactions and their anti-proliferative activity, Journal of combinatorial chemistry 12(1) (2010) 20-24.

[29] G.C. Nandi, S. Samai, R. Kumar, M. Singh, An efficient one-pot synthesis of tetrahydrobenzo [a] xanthene-11-one and diazabenzo [a] anthracene-9, 11-dione derivatives under solvent free condition, Tetrahedron 65(34) (2009) 7129-7134.

[30] J. Li, L. Lu, W. Su, A new strategy for the synthesis of benzoxanthenes catalyzed by proline triflate in water, Tetrahedron Letters 51(18) (2010) 2434-2437.

[31] J. Li, W. Tang, L. Lu, W. Su, Strontium triflate catalyzed one-pot condensation of β-naphthol, aldehydes and cyclic 1, 3-dicarbonyl compounds, Tetrahedron Letters 49(50) (2008) 7117-7120.

[32] G.P. Lu, C. Cai, A facile, one-pot, green synthesis of polysubstituted 4H-pyrans via piperidine-catalyzed three-component condensation in aqueous medium, Journal of Heterocyclic Chemistry 48(1) (2011) 124-128.

[33] S. Ko, C.-F. Yao, Heterogeneous catalyst: Amberlyst-15 catalyzes the synthesis of 14-substituted-14H-dibenzo [a, j] xanthenes under solvent-free conditions, Tetrahedron Letters 47(50) (2006) 8827-8829.

[34] H.R. Shaterian, M. Ghashang, N. Mir, Aluminium hydrogensulfate as an efficient and, Arkivoc 15 (2007) 1-10.

[35] B. Rajitha, B.S. Kumar, Y.T. Reddy, P.N. Reddy, N. Sreenivasulu, Sulfamic acid: a novel and efficient catalyst for the synthesis of aryl-14H-dibenzo [aj] xanthenes under conventional heating and microwave irradiation, Tetrahedron Letters 46(50) (2005) 8691-8693.

[36] A. Khoramabadi-zad, S.-A. Akbari, A. Shiri, H. Veisi, One-pot synthesis of 14H-dibenzo [a, j] xanthene and its 14-substituted derivatives, Journal of Chemical Research 2005(5) (2005) 277-279.

[37] S.B. Patil, R.P. Bhat, S.D. Samant, Cation-Exchange Resins: Efficient Heterogeneous Catalysts for Facile Synthesis of Dibenzoxanthene from β-Naphthol and Aldehydes, Synthetic Communications 36(15) (2006) 2163-2168.

[38] P. Salvi, A. Mandhare, A. Sartape, D. Pawar, S.-H. Han, S. Kolekar, An efficient protocol for synthesis of tetrahydrobenzo [b] pyrans using amino functionalized ionic liquid, Comptes Rendus Chimie 14(10) (2011) 878-882.

[39] R. Ballini, G. Bosica, M.L. Conforti, R. Maggi, A. Mazzacani, P. Righi, G. Sartori, Three-component process for the synthesis of 2-amino-2-chromenes in aqueous media, Tetrahedron 57(7) (2001) 1395-1398.

[40] T.-S. Jin, J.-C. Xiao, S.-J. Wang, T.-S. Li, Ultrasound-assisted synthesis of 2-amino-2-chromenes with cetyltrimethylammonium bromide in aqueous media, Ultrasonics Sonochemistry 11(6) (2004) 393-397.

[41] X.s. Wang, D.q. Shi, H.z. Yu, G.f. Wang, S.j. Tu, Synthesis of 2-Aminochromene Derivatives Catalyzed by KF/Al2O3, Synthetic communications 34(3) (2004) 509-514.

[42] M.R. Naimi-Jamal, S. Mashkouri, A. Sharifi, An efficient, multicomponent approach for solvent-free synthesis of 2-amino-4H-chromene scaffold, Molecular diversity 14(3) (2010) 473-477.

[43] S. Balalaie, S. Ramezanpour, M. Bararjanian, J.H. Gross, DABCO-catalyzed efficient synthesis of naphthopyran derivatives via One-Pot three-component condensation reaction at room temperature, Synthetic Communications 38(7) (2008) 1078-1089.

[44] J. Heddle, A. Maxwell, Quinolone-binding pocket of DNA gyrase: role of GyrB, Antimicrobial agents and chemotherapy 46(6) (2002) 1805-1815.

[45] R. Kumar, B.S. Madhumathi, V. Nagaraja, Molecular basis for the differential quinolone susceptibility of mycobacterial DNA gyrase, Antimicrobial agents and chemotherapy 58(4) (2014) 2013-2020.

[46] T.-S. Jin, J.-C. Xiao, S.-J. Wang, T.-S. Li, X.-R. Song, An efficient and convenient approach to the synthesis of benzopyrans by a three-component coupling of one-pot reaction, Synlett 2003(13) (2003) 2001-2004.

[47] M.M. Heravi, F. Derikvand, M. Haghighi, K. Bakhtiari, " On Water": Rapid Knoevenagel Condensation Using Sodium Pyruvate, Letters in Organic Chemistry 3(4) (2006) 297-299.

[48] M. Paesha, V. Jayäshankara, An efficient synthesis of 2-aminobenzochromene derivatives catalysed by tetrabutylammoniumbromide (TBABr) under microwave irradiation in aqueous medium, (2007).

[49] A. Patra, T. Mahapatra, Intramolecular Heck Reaction on Bromobenzyloxy-Substituted Chromenes: Formation of Chelated Ketones, Synthetic Communications 43(11) (2013) 1602-1609.

[50] G. Shanthi, P.T. Perumal, An eco-friendly synthesis of 2-aminochromenes and indolyl chromenes catalyzed by InCl3 in aqueous media, Tetrahedron Letters 48(38) (2007) 6785-6789.

[51] X.-S. Wang, G.-S. Yang, G. Zhao, Enantioselective synthesis of naphthopyran derivatives catalyzed by bifunctional thiourea-tertiary amines, Tetrahedron: Asymmetry 19(6) (2008) 709-714.

[52] L. Chen, X.-J. Huang, Y.-Q. Li, M.-Y. Zhou, W.-J. Zheng, A one-pot multicomponent reaction for the synthesis of 2-amino-2-chromenes promoted by N, N-dimethylamino-functionalized basic ionic liquid catalysis under solvent-free condition, Monatshefte für Chemie-Chemical Monthly 140(1) (2009) 45.

[53] S. Qadir, A.A. Dar, K.Z. Khan, Synthesis of biscoumarins from 4-hydroxycoumarin and aromatic aldehydes—a comparative assessment of percentage yield under thermal and microwave-assisted conditions, Synthetic Communications® 38(20) (2008) 3490-3499.

[54] M. Kidwai, V. Bansal, P. Mothsra, S. Saxena, R.K. Somvanshi, S. Dey, T.P. Singh, Molecular iodine: A versatile catalyst for the synthesis of bis (4-hydroxycoumarin) methanes in water, Journal of Molecular Catalysis A: Chemical 268(1-2) (2007) 76-81.

[55] A. Shaabani, S. Samadi, Z. Badri, A. Rahmati, Ionic liquid promoted efficient and rapid one-pot synthesis of pyran annulated heterocyclic systems, Catalysis letters 104(1-2) (2005) 39-43.

[56] J.F. Roudier, A. Foucaud, A convenient synthesis of 4H-chromenes, Synthesis (Stuttgart) (2) (1984) 159-160.

[57] H.-J. Wang, J. Lu, Z.-H. Zhang, Highly efficient three-component, one-pot synthesis of dihydropyrano [3, 2-c] chromene derivatives, Monatshefte für Chemie-Chemical Monthly 141(10) (2010) 1107-1112.

[58] J.M. Khurana, S. Kumar, Tetrabutylammonium bromide (TBAB): a neutral and efficient catalyst for the synthesis of biscoumarin and 3, 4-dihydropyrano [c] chromene derivatives in water and solvent-free conditions, Tetrahedron Letters 50(28) (2009) 4125-4127.

[59] R. Ghorbani-Vaghei, R. Karimi-Nami, Z. Toghraei-Semiromi, M. Amiri, M. Ghavidel, One-pot synthesis of aliphatic and aromatic 2H-indazolo [2, 1-b] phthalazine-triones catalyzed by N-halosulfonamides under solvent-free conditions, Tetrahedron 67(10) (2011) 1930-1937.

[60] S. Paul, P. Bhattacharyya, A.R. Das, One-pot synthesis of dihydropyrano [2, 3-c] chromenes via a three component coupling of aromatic aldehydes, malononitrile, and 3-hydroxycoumarin catalyzed by nano-structured ZnO in water: a green protocol, Tetrahedron letters 52(36) (2011) 4636-4641.

[61] T.-S. Jin, A.-Q. Wang, X. Wang, J.-S. Zhang, T.-S. Li, A clean one-pot synthesis of tetrahydrobenzo [b] pyran derivatives catalyzed by hexadecyltrimethyl ammonium bromide in aqueous media, Synlett 2004(05) (2004) 0871-0873.

[62] S. Gao, C.H. Tsai, C. Tseng, C.-F. Yao, Fluoride ion catalyzed multicomponent reactions for efficient synthesis of 4H-chromene and N-arylquinoline derivatives in aqueous media, Tetrahedron 64(38) (2008) 9143-9149.

[63] S.-J. Tu, Y. Gao, C. Guo, D. Shi, Z. Lu, A convenient synthesis of 2-amino-5, 6, 7, 8-tetrahydro-5-oxo-4-aryl-7, 7-dimethyl-4H-benzo-[b]-pyran-3-carbonitrile under microwave irradiation, Synthetic communications 32(14) (2002) 2137-2141.

[64] L.-M. Wang, J.-H. Shao, H. Tian, Y.-H. Wang, B. Liu, Rare earth perfluorooctanoate [RE (PFO) 3] catalyzed one-pot synthesis of benzopyran derivatives, Journal of fluorine chemistry 127(1) (2006) 97-100.

[65] S. Balalaie, M. Bararjanian, A.M. Amani, B. Movassagh, (S)-Proline as a neutral and efficient catalyst for the one-pot synthesis of tetrahydrobenzo [b] pyran derivatives in aqueous media, Synlett 2006(02) (2006) 263-266.

[66] A.T. Khan, M. Lal, S. Ali, M.M. Khan, One-pot three-component reaction for the synthesis of pyran annulated heterocyclic compounds using DMAP as a catalyst, Tetrahedron letters 52(41) (2011) 5327-5332.

[67] Y. Sarrafi, E. Mehrasbi, A. Vahid, M. Tajbakhsh, Well-ordered mesoporous silica nanoparticles as a recoverable catalyst for one-pot multicomponent synthesis of 4H-chromene derivatives, Chinese Journal of Catalysis 33(9-10) (2012) 1486-1494.

[68] D.R. Koes, M.P. Baumgartner, C.J. Camacho, Lessons learned in empirical scoring with smina from the CSAR 2011 benchmarking exercise, Journal of chemical information and modeling 53(8) (2013) 1893-1904.

[69] R.R. Nasab, F. Hassanzadeh, G.A. Khodarahmi, M. Rostami, M. Mirzaei, A. Jahanian-Najafabadi, M. Mansourian, Docking study, synthesis and antimicrobial evaluation of some novel 4-anilinoquinazoline derivatives, Research in pharmaceutical sciences 12(5) (2017) 425.

[70] R. Huey, G.M. Morris, A.J. Olson, D.S. Goodsell, A semiempirical free energy force field with charge-based desolvation, Journal of computational chemistry 28(6) (2007) 1145-1152.

[71] F. Shiri, A. Shahraki, M. Nejati-Yazdinejad, 3D-QSAR and Molecular Docking Study on Maleimide-Based Glycogen Synthase Kinase 3 (GSK-3) Inhibitors as Stimulators of Steroidogenesis, Polycyclic Aromatic Compounds (2018) 1-15.

[72] E. Nazarshodeh, F. Shiri, J.B. Ghasemi, 3D-QSAR and virtual screening studies in identification of new Rho kinase inhibitors with different scaffolds, Journal of the Iranian Chemical Society 12(11) (2015) 1945-1959.

[73] T. Sander, J. Freyss, M. von Korff, C. Rufener, DataWarrior: an open-source program for chemistry aware data visualization and analysis, Journal of chemical information and modeling 55(2) (2015) 460-473.